https://doi.org/10.5194/egusphere-2024-3554
Preprint. Discussion started: 20 November 2024

Ionospheric Chaos in Solar quiet Current due to Sudden Stratospheric Warming Events Across Europe-Africa Sector

Irewola Aaron, Oludehinwa[1,2,*]; Andrei, Velichko[3]; Olasunkanmi Isaac, Olusola[2]; Olawale Segun, Bolaji[3,6]; Norbert, Marwan[4]; Babalola Olasupo, Ogunsua[5,7]; Abdullahi Ndzi, Njah[3]; Timothy Oluwaseyi Ologun[7].

1. Department of Physics, Caleb University, Lagos, Nigeria
2. Department of Physics, University of Lagos, Lagos, Nigeria
3. Institute of Physics and Technology, Petrozavodsk State University, 185910 Petrozavodsk, Russia.
4. Research Department of Complexity Science, Potsdam Institute for Climate Impact Research (PIK), Member of the Leibniz Association, 14412 Potsdam, Germany.
5. Key Laboratory for middle Atmospheric and Global Environment Observation (LAGEO), Institute of Atmospheric Physics (IAP), Chinese Academy of Science, Beijing, China.
6. Department of Physics, University of Tasmania, Australia.
7. Department of Physics, Federal University of Technology, Akure, Nigeria.

*Corresponding-Author:

irewola.oludehinwa@calebuniversity.edu.ng; or Irewola2012@yahoo.com

Tel.: +2348068030109

Abstract

This study examines the ionospheric chaos in the solar quiet current, across Europe and Africa sectors during 2009 and 2021 Sudden Stratospheric Warming (SSW). The SSW was categorized into precondition, ascending, peak, descending, after and no-SSW phases based on the rising stratospheric temperature. Thirteen magnetometer stations, located within the geographical longitude of 26° to 40° across Europe and Africa sectors were considered. The magnetometer data obtained during the periods of SSW were used to derived the ionospheric solar quiet current time series. This solar quiet current time series was transformed into a complex network representation using the Horizontal Visibility Graph (HVG) approach and Fuzzy Entropy was employed on the

https://doi.org/10.5194/egusphere-2024-3554
Preprint. Discussion started: 20 November 2024

transformed solar quiet current time series to quantify the presence ionospheric chaos during the periods of SSW. The results revealed that the latitudinal distribution of entropy depicts high entropy values indicating the presence of ionospheric chaos in most of the stations situated within the European sector compared to stations in the African sector. A consistent low entropy values unveiling the presence of orderliness behavior was found to be prominent in the Africa sector. This dominance of orderliness behavior in the Africa sector during SSW means that the influence of SSW on the regional ionosphere of this sector is minimal. However, the pronounced features of ionospheric chaos found in the European sector reveal evidence of significant effects of SSW on the regional ionosphere in this sector. Finally, we found that after the peak phase of SSW, the ionospheric chaos is more pronounced.

Keywords: Sudden Stratospheric Warming (SSW), Solar quiet current Sq(H), Ionospheric chaos, Fuzzy Entropy, Horizontal Visibility Graph (HVG)

1. Introduction.

Natural systems, including the troposphere, stratosphere, and ionosphere, are significantly affected by regional climate changes, particularly temperature increases (Li et al., 2023; Fortin, 2017). As the temperature rises, there are a wide range of effects on weather conditions. For instance, less snowpack in mountain ranges and polar areas is experienced as a result of climate change and the snow melts faster (Williams et al., 2024; Fortin, 2017). The increasing number of extreme weather events is caused by climate change. Climate change does also impact the frequent occurrence of sudden stratospheric warming (SSW), with the consequence of communication disruptions, economic disruptions, transportation disruption and energy demand fluctuations (Yasyukevich et al., 2022; Li et al., 2023; Wright et al., 2021; Baldwin et al., 2021). The emergence of SSW is described by an atmospheric phenomenon where the stratospheric temperature increases rapidly

https://doi.org/10.5194/egusphere-2024-3554
Preprint. Discussion started: 20 November 2024

within a couple of days (>30 to 40k). SSW is one of the usual meteorological events, where the stratospheric temperature increases rapidly in the winter polar region due to the rapid growth of quasi-stationary planetary waves (Baldwin et al., 2021; Butler et al., 2015). These quasi-stationary planetary waves interact nonlinearly with the atmospheric tides, leading to the generation of both migrating and non-migrating tidal components (Wang et al., 2021, 2023; Antokhina et al., 2023; Ern et al., 2021; Liu et al., 2010; Chau et al., 2012). During SSW, the planetary waves and tidal interaction can generate electromotive force that drive the electric currents and move the electrical conducting air in the ionosphere across the earth's magnetic field (Siddiqui et al., 2018; Yamazaki et al., 2020; Yamazaki, 2014; Wagner et al., 1980; Richmond, 1989; Yamazaki and Maute, 2017; Yamazaki and Richmond, 2013). It has been reported that during SSW, the coupling processes at lower atmosphere can propagate forcing that can reshape the plasma density variability of the ionosphere. These reshape in ionospheric plasma possesses some dynamical characteristics that are of nonlinear nature. The main mechanism responsible for the connections of this influences includes planetary waves, atmospheric tides, and gravity waves (Goncharenko et al., 2021; Chau et al., 2012; Goncharenko et al., 2010, 2012; Yiğit et al., 2024; Zhou et al., 2023; Gordiyenko et al., 2024; Klimenko et al., 2018, 2019; Gómez-Escolar et al., 2014).

In the upper atmosphere, high energy injections into the ionosphere due to the solar wind-magnetosphere coupling processes during geospace disturbances such as geomagnetic storms, HILDCAAs and others are considered to be the major factors influencing the dynamics of the ionosphere (Zou et al., 2014; Hajra et al., 2015; Tsurutani et al., 2020; Raeder et al., 2016; Oludehinwa et al., 2023; Lin et al., 2022). However, (Goncharenko et al., 2010) and others have demonstrated that the reshaping of electron density variability during SSWs is similar in magnitude to that of moderate geomagnetic storms. Therefore, the occurrence of SSW can infer a

https://doi.org/10.5194/egusphere-2024-3554
Preprint. Discussion started: 20 November 2024

phenomenon where the ionospheric plasma density is reshaped and destabilized, thereby posing an operational hazard on radio communication, navigation, and imaging system.

This calls for the need to examine the state of the ionosphere during SSW by investigating the dynamics of the ionospheric current system during quiet periods as SSW emerges. Notably, the dynamics of the ionospheric current changes with time. They exhibit complex fluctuations in form of nonlinear behavior due to their continuous interactions in response to lower atmospheric circulation and the energy deposition of solar wind-magnetosphere coupling processes. The ionospheric currents during these meteorological and space weather events are propelling phenomena that can unveil the connections between the lower atmosphere and upper atmosphere (Pedatella and Forbes, 2010; Liu et al., 2010; Eswaraiah et al., 2017). According to the dynamo theory, the neutral wind (U) in the dynamo region transports conducting plasma across the Earth's magnetic fields (B), generating electric fields and currents that flow in the E-region of the ionosphere (Wagner et al., 1980; Yamazaki and Richmond, 2013; Yamazaki et al., 2012b). This ionospheric current system during geomagnetically quiet periods is referred to as Solar quiet Sq(H) currents.

The ionospheric response to SSW introduces spatial and temporal variability in the dynamics of the ionospheric current system and exhibits complex fluctuation signatures in its underlying dynamics, which require further investigation. In addition, the research question of the contribution of SSW formation to the regional ionosphere across the European-African sector needs special attention. This observation forms the basis of this study to quantitatively examine the dynamics of the ionospheric solar quiet current Sq(H) before its orderly and disorderly (chaotic) behavior during the anomalous stratospheric temperature changes over the Europe-Africa sector. The present study seeks to unravel the ionospheric chaotic dynamics in the solar quiet current Sq(H)

https://doi.org/10.5194/egusphere-2024-3554
Preprint. Discussion started: 20 November 2024

due to the emerging influence of the SSW over this sector. Also, to reveal the common features of the ionospheric dynamics due to the occurrence of SSWs during solar minimum years.

Several studies have already investigated the solar quiet current during SSW (Yamazaki, 2014; Bolaji et al., 2016a; Charles Owolabi and Babatunde Rabiu and Kayode Oluyo, 2015; Bolaji et al., 2015; Yamazaki and Maute, 2017; Yamazaki et al., 2011). (Fejer et al., 2011) studied the evidence of possible equatorial vertical plasma drifts associated with SSW. They found a strongly enhanced lunar semi-diurnal vertical plasma drift amplitude during early morning solar flux warming. (Maute et al., 2014) also found evidence of ionospheric vertical drift changes during SSW and attribute these drift changes to the interaction of specific tides and planetary waves. (Yamazaki et al., 2012a) examined the ionospheric current system during SSW of 2002 and 2003 considering the Northern and Southern Hemisphere across the east Asia region. They reported an additional current system that would be superposed on the normal Sq current system and further suggest that abnormally large lunar tidal winds played the main role in producing the additional current and counter electrojet (CEJ). (Yamazaki et al., 2012b) further looked at the solar quiet current during SSW. They noticed a significant decrease and increase in the intensity of the solar quiet current in the Northern and Southern Hemispheres, respectively, with a decrease in the longitudinal separation between the Northern and Southern eddies. (Yamazaki, 2014) examined solar and lunar ionospheric tidal drives, which are thought to cause ionospheric electrodynamics effects during SSW, by estimating the average solar and lunar ionospheric current systems for SSW and non-SSW periods. He found that the lunar current intensity is enhanced during SSWs by approximately 75% while the solar current intensity is much smaller by approximately 10%. (Bolaji et al., 2016b) reported the solar quiet current response in the Africa sector. They categorized the rising stratospheric temperature during SSW into six phases (precondition, ascending, peak, descending,

https://doi.org/10.5194/egusphere-2024-3554
Preprint. Discussion started: 20 November 2024

after and no) and noticed a counter electrojet (CEJ) after the polar stratospheric temperature reached its maximum value (SSW peak). In addition, a decrease in the Sq(H) magnitude was observed at geomagnetic latitudes between 21.13°N (Fayum) in Egypt and 39.51°S (Durban) in South Africa. (Siddiqui et al., 2018) investigated the evidence for an Equatorial Electrojet (EEJ) during a major SSW event. They found a significant increase in the amplitude of the EEJ semidiurnal lunar tides during all major SSW events investigated. The mechanism responsible for the anomalies in the tropical lower thermosphere-ionosphere due to SSW 2009 was demonstrated by (Klimenko et al., 2019). The authors claim that perturbations in the ionospheric conductivity also make a significant contribution to the formation of the electric field response to SSW. They also show that the phase change of the semidiurnal migrating solar tide (SW2) in the neutral wind caused by the 2009 SSW at the altitude of the dynamo electric field generation has a crucial importance for the SW2 phase change in the zonal electric field.

Notably, one of the atmospheric activities unveiling the coupling features between the lower and upper atmospheric circulation is the dynamics of the ionospheric current system (Yamazaki et al., 2012b; Bolaji et al., 2016b; Yamazaki and Richmond, 2013). The ionospheric current system is a key factor that can reveal the dynamical characteristics of the ionosphere during SSW. Interestingly, among all the aforementioned studies on ionospheric currents during SSW events, it is noteworthy that these currents have not been examined from the aspect of chaos theory. Since then, it has been reported that the lower and middle atmospheric circulation (i.e. troposphere-stratosphere coupling) nonlinearly interact during SSW, modulating the dynamics of the ionosphere. Therefore, this nonlinearity (out-of-equilibrium) features is the prevailing condition for the existence of chaotic behavior in the ionosphere. Important characteristics of chaotic behavior are the existence of a strange attractor and that a small change in the ionosphere due to

https://doi.org/10.5194/egusphere-2024-3554
Preprint. Discussion started: 20 November 2024

SSW can amplify the dynamics, leading to instability and divergence from its initial state (Takens, 1981). Additionally, the ionosphere is considered a dynamical system due to its continuous response to atmospheric forcing. Bifurcation behaviour within the ionospheric system is eminent (Hysell, 2020; Lapenta, 2020; Materassi, 2020). In some occasions, the ionospheric dynamics tend to exhibit either orderliness or disorderliness (chaotic) behavior in its underlying dynamics due to influences of atmospheric forces from lower and upper atmospheric circulations. Therefore, it is crucial to examine the dynamics of the ionospheric current system during quiet periods as the stratospheric temperature rises during SSW. Implementing the concept of nonlinear dynamics, informed by information theory and graph theory, presents an innovative approach to reveal the contributions of SSW to the ionospheric region across the Europe and Africa sectors. Therefore, this study focuses on the ionospheric chaos (order-disorder behavior) in the ionospheric current system during quiet periods when the stratospheric temperature increases anomalously.

In this context, a theoretically robust method known as the Horizontal Visibility graph (HVG), derived from graph theory, is employed to preprocess the solar quiet current time series, while the ionospheric chaos during SSW is revealed through Fuzzy Entropy (FuzzyEn). HVG and FuzzyEn have been demonstrated to be useful tools in inter-disciplinary applications and when analyzing challenging data (Conejero et al., 2024; O'Pella, 2019; Gonçalves et al., 2016; Simons et al., 2018; Velichko et al., 2023, 2022; Velichko and Heidari, 2021).

1.1 Characterization of 2009 and 2021 Major SSW Events

The 2009 SSW event occurred from January to March. Its rising stratospheric temperature and the corresponding stratospheric zonal mean wind was categorized into six phases during these periods: SSW Pre-Condition Phase, SSW Ascending Phases, SSW Peak Phase, SSW Descending Phase,

https://doi.org/10.5194/egusphere-2024-3554
Preprint. Discussion started: 20 November 2024

After SSW Phase, and No SSW phase (Figure (1)). The red color represents the stratospheric mean air temperature (k) at 10hPa. While the black color is the stratospheric zonal mean wind at 10hPa.

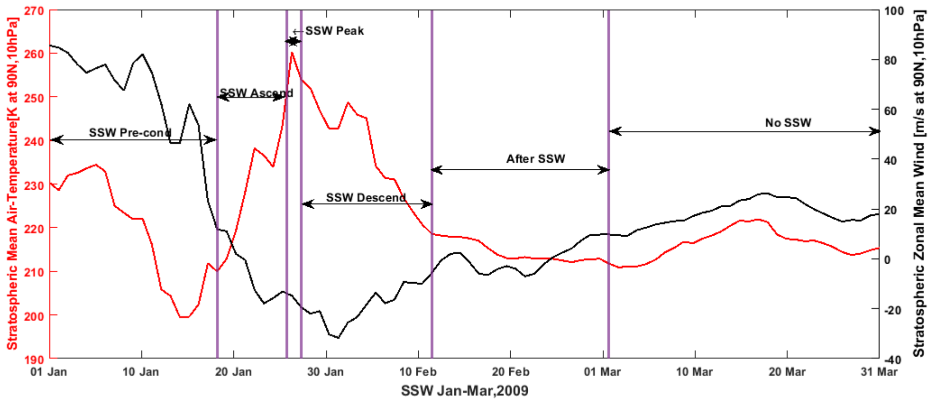

Figure 1: The stratospheric zonal mean air temperature and zonal mean wind occurring January-March, 2009 showing the SSW Precondition Phase, SSW Ascending Phase, SSW peak Phase, SSW Descending Phase, After SSW Phase and no SSW phase.

The SSW precondition phase represents the start of the increase in the stratospheric temperature (1-16 January) shown in Figure 1, the SSW ascending phase signifies when the stratospheric temperature increases (17-21 January), the SSW peak phase is when the stratospheric temperature reaches its maximum (22-24 January), the SSW Descending phase indicates the begin of the stratospheric temperature decline (25 January-12 February), the After SSW phase represents when the stratospheric temperature begins to recover to its normal state (13 February-2 March), and the No SSW phase represents when the stratospheric temperature finally recovers to its normal state (3-31 March). The SSW event was categorized in accordance to the work of (Bolaji et al., 2016b).

The stratospheric temperature and its corresponding zonal mean wind for the 2021 SSW event is shown in Figure 2. The SSW occurred from December 2020 to February 2021 and was also

https://doi.org/10.5194/egusphere-2024-3554
Preprint. Discussion started: 20 November 2024

categorized into six phases. The SSW precondition phase spans between 1 and 27 December, 2020, the SSW ascending phase is from 28 December 2020 to 2 January 2021, while the SSW peak phase ranges from 3-5 January 2021, the SSW descending phase spans within 6-14 January 2021, and the After-SSW phase is from 15 January-16 February 2021. Finally, the No SSW phase emerges from 17-28 February 2021.

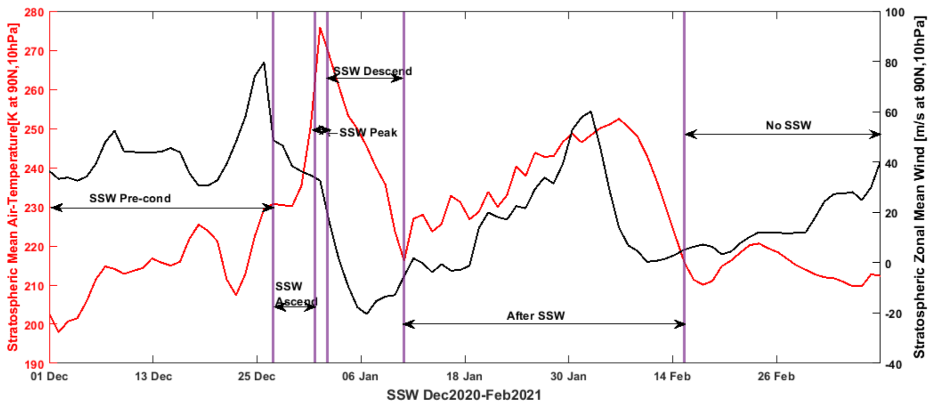

Figure 2: The stratospheric zonal mean air temperature and zonal mean wind from December 2020 until February, 2021 revealing the SSW Precondition Phase, SSW Ascending Phase, SSW peak Phase, SSW Descending Phase, After SSW Phase and no SSW phase.

1.2 Global Scale of geomagnetic activities during the 2009 and 2021 SSW Events

The year 2009 was the beginning of a solar minimum of the solar cycle 24 while the year 2021 was a solar minimum at the end of the solar cycle 24. Generally, solar minimum years are periods, where the geomagnetic disturbances mostly record quiet periods. This indicates that the years 2009

https://doi.org/10.5194/egusphere-2024-3554
Preprint. Discussion started: 20 November 2024

and 2021 of solar cycle 24 are periods where the geomagnetic disturbances were minimal.

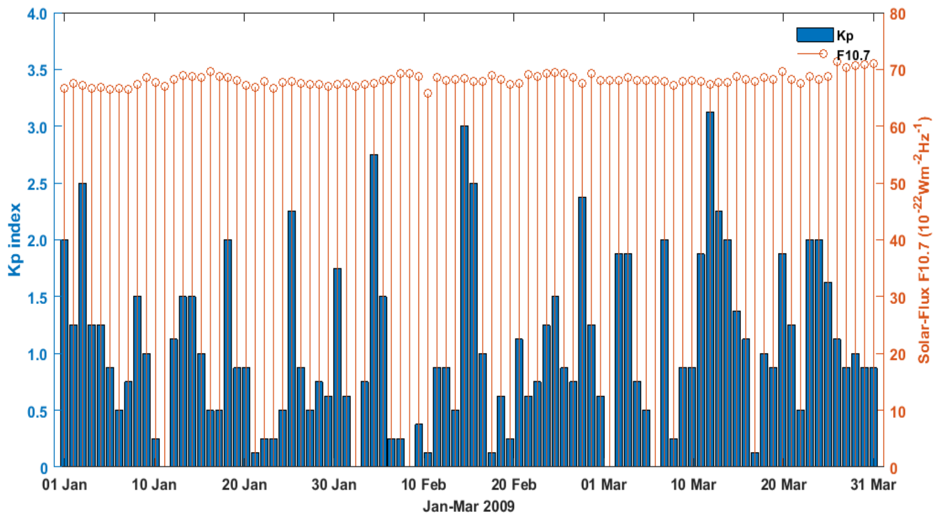

Figure 3: The planetary index K_p (blue bars) and Solar flux $F_{10.7}$ (red lines) from January to March, 2009.

The planetary index (K_p) and the solar flux activity during the months of 2009 and 2021 SSW event are shown in Figures (3 & 4) respectively. During the 2009 SSW event (January-March), the planetary index (K_p) recorded values of $K_p \leq 2^+$, while the solar flux index ($F_{10.7}$) was around $F_{10.7}$~72 (Figure (3)). Notably, the planetary index and solar flux activity recorded low values indicating that the geomagnetic activities were quiet.

https://doi.org/10.5194/egusphere-2024-3554
Preprint. Discussion started: 20 November 2024

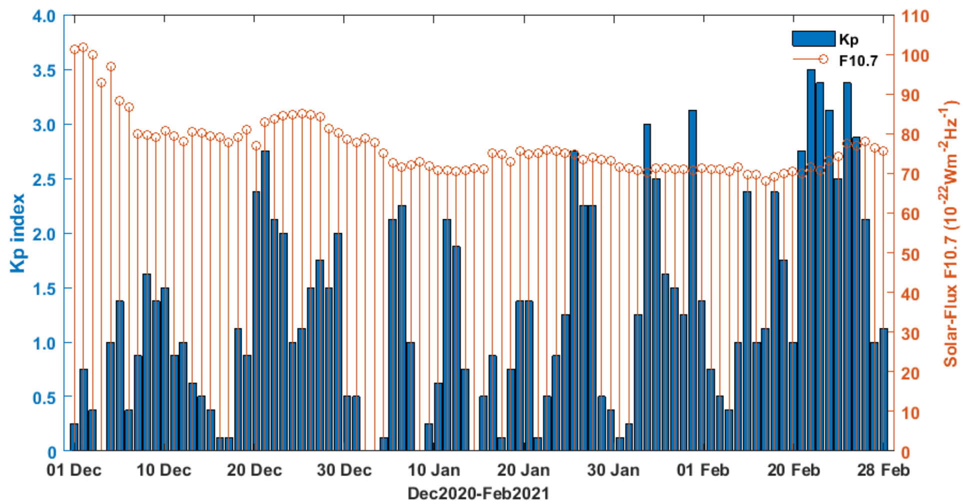

Figure 4: The planetary index: K_p (blue bar) and Solar flux $F_{10.7}$ (red lines) from December 2020-February, 2021.

Also, the planetary index during the occurrence of the 2021 SSW (December 2020-February 2021) was within $K_p \leq 3^+$ and the solar flux activity was within $F_{10.7}$~100 (Figure 4). This further indicates that the geomagnetic activities during the periods of 2009 and 2021 SSW occurrences were quiet. This observed characteristic testifies the uniqueness of the selected SSW events in 2009 and 2021. Examining the ionospheric chaos in solar quiet currents during periods of minimal solar and geomagnetic activity will unveil the contributing influence of SSW on ionospheric dynamics across the Europe and Africa sector.

https://doi.org/10.5194/egusphere-2024-3554
Preprint. Discussion started: 20 November 2024

2. Data Acquisition and Method of Analysis

Ground-based magnetometer data acquired from the Magnetic Data Acquisition System (MAGDAS) at the International Research Centre for Space and Planetary Environment Science ($i - SPES$), Fukuoka, Japan (http://magdas2.serc.kyushu-u.ac.jp/) was used in this study. The geographical location of the studied areas is shown in Figure 5.

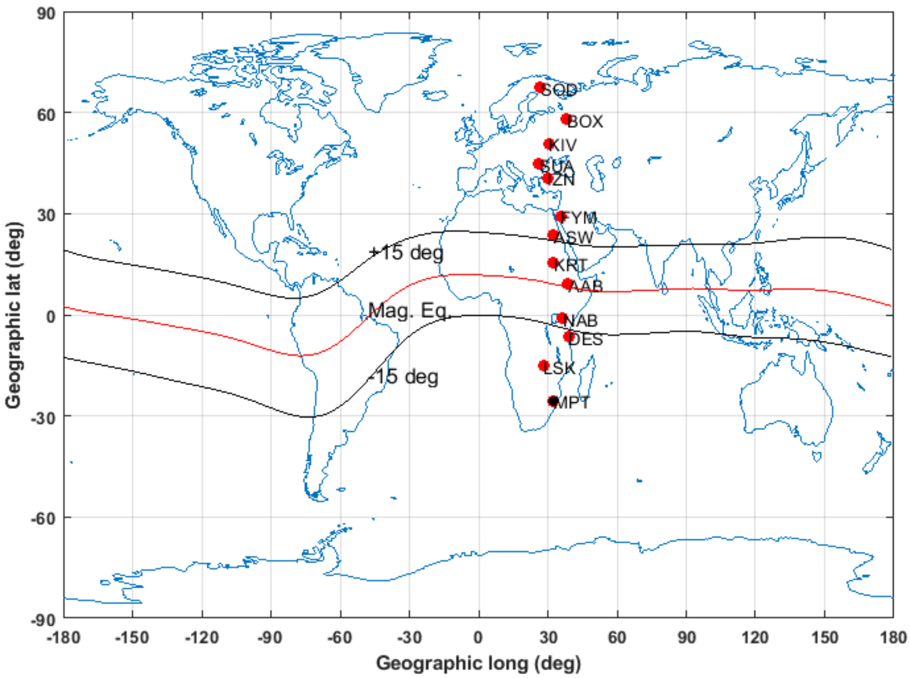

Figure 5: The geographical location of the magnetometer observatories stations investigated across the Europe and Africa sector.

The acquired magnetic data from MAGDAS covers 8 magnetometer stations situated in the Africa sector distributed within the geographical latitudes of both Northern and Southern Hemisphere shown in Table 1.

https://doi.org/10.5194/egusphere-2024-3554
Preprint. Discussion started: 20 November 2024

TABLE 1: STATIONS INVESTGATED ACROSS EUROPE AND AFRICA SECTOR

S/ No	Stations	Country	Geographical latitude	Geographical Longitude	Geomagnetic Latitude	Geomagnetic Longitude	Local Time (LT)	Magnetometer Network
1	Sodankyla (SOD)	Finland	67.37	26.63	63.70	107.68	UTC+3	INTERMAGNET
2	Borok (BOX)	Russia	58.07	38.23	53.92	113.32	UTC+3	INTERMAGNET
3	Kiev Dymer (KIV)	Ukraine	50.70	30.30	46.32	104.39	UTC+3	INTERMAGNET
4	Surlari (SUA)	Romania	44.68	26.25	39.52	99.52	UTC+3	INTERMAGNET
5	Iznik (IZN)	Turkey	40.50	29.72	34.74	102.13	UTC+3	INTERMAGNET
6	Fayum (FYM)	Egypt	29.18	35.50	21.78	106.00	UTC+2	MAGDAS
7	Aswan (ASW)	Egypt	23.50	32.51	14.56	103.89	UTC+2	MAGDAS
8	Khartoum (KRT)	Sudan	15.33	32.32	5.69	103.80	UTC+2	MAGDAS
9	Addis Ababa (AAB)	Ethiopia	9.01	38.74	0.14	110.46	UTC+3	MAGDAS
10	Nairobi (NAB)	Kenya	-1.10	36.48	-10.58	108.18	UTC+3	MAGDAS
11	Dar es Salaam (DES)	Tanzania	-6.80	39.28	-16.26	110.72	UTC+3	MAGDAS
12	Lusaka (LSK)	Zambia	-15.23	28.19	-26.06	98.31	UTC+2	MAGDAS
13	Maputo (MPT)	Mozambique	-25.50	32.36	-35.92	99.56	UTC+2	MAGDAS

Also, magnetometer observations across Europe were acquired from the International Real-time Magnetic Observatory Network (INTERMAGNET) (available online at www.intermagnet.org). The collection consists of 5 magnetometer observatory stations across Europe, see Table 1. The magnetometer data were acquired during the periods of the 2009 and 2021 SSW occurrences.

The planetary (K_p) index during 2009 and 2021 SSW periods was downloaded from GFZ Indices of Global Geomagnetic Activity (https://www.gfz-potsdam.de/Kp-index/) while the Solar flux activity ($F_{10.7}$) at 2009 and 2021 SSW periods were collected online from the archive of the Space Physics Data Facility, NASA (https://omniweb.gsfc.nasa.gov/form/dx1.html).

The daily mean values of zonal mean air temperature and wind during the periods of 2009 and 2021 SSW were acquired from the National Oceanic and Atmospheric Administration (NOAA)

https://doi.org/10.5194/egusphere-2024-3554
Preprint. Discussion started: 20 November 2024

(https://psl.noaa.gov/data/getpage/). The ionospheric solar quiet currents, Sq(H), was derived using the H-component of the magnetic field data with daily resolution (with time unit in minutes).

2.1 Ionospheric Solar Quiet Current Sq(H) as Observational Time Series

The dynamics of the Sq(H) current system changes in its daily variation in sequence with time. As a result of its changes in dynamical behavior, the Sq(H) current can be regarded as an observational time series data. To derive the daily dynamics of the Sq(H) current, magnetic field data from various magnetometer stations across Europe and Africa, within the geographical longitude range of 26° to 40°, were archived at one-minute intervals. The H-component (magnetic northward) was collected in minutes from all the stations under investigation and the values of the geomagnetic storm index in minutes (SYM-H) were subtracted from the H-component to minimize the disturbance field arising from magnetospheric currents (Yamazaki et al., 2012b; Bolaji et al., 2016b; Yamazaki et al., 2012a). The derivation of the Sq(H) current is mathematically expressed as:

$$\Delta H_{ground} = H_{local} - (SYMH\cos(L)) \qquad (1)$$

where $SYMH\cos(L)$ is the calculated disturbance field arising from the magnetospheric current effect and L is the geomagnetic latitude of the stations under investigation.

To estimate the solar quiet current, the average value between 24:00 and 1:00 local time (LT) in minutes for a particular day was calculated.

$$BLV = \frac{\Delta H_{01} + \Delta H_{24}}{2} \qquad (2)$$

The notation ΔH_{01} and ΔH_{24} are the 60 minutes values of H component at 1:00 and 24:00 LT while BLV is the Baseline.

https://doi.org/10.5194/egusphere-2024-3554
Preprint. Discussion started: 20 November 2024

The residual value after subtracting the baseline value from the H-component gives the solar quiet current time series considered in minutes.

$$S_q(H)_t = H_t - BLV \tag{3}$$

$S_q(H)_t$ is the solar quiet current considered in minutes. The analysis of the Sq(H) was deduced for day-to-day activities of the 2009 SSW (January-March) and 2021 SSW (December 2020-Februay) periods for all stations under investigation.

2.2 Detrending of Solar quiet Sq(H) Current Time Series by Horizontal Visibility Graph (HVG).

HVG is a simplified visibility graph that transforms a time series into a graph structure maintaining the inherent characteristics of the transformed time series (Conejero et al., 2024; Gonçalves et al., 2016; O'Pella, 2019; Luque et al., 2009; Zou et al., 2019). It considers the time series in a two-dimensional plane and determines which data are mutually visible. Each value in the time series data is represented by a vertical bar. Two data points share visibility if a line can be drawn from one bar to the other without intersecting any other vertical bars between them. Transforming the signal via HVG, we obtain a graph where nodes represent points in the signals, and the connection between them are based on horizontal visibility. This transformation allows for a shift from a time series to a graph structure while preserving topological information about the signal's structure, making it useful for analyzing the dynamic properties of time series data.

Let us consider a time series of *N*-data points be represented as:

$$[x_i, i = 1,2, \dots, N] \tag{4}$$

https://doi.org/10.5194/egusphere-2024-3554
Preprint. Discussion started: 20 November 2024

Two nodes i and j in the graph are connected, if it is possible to trace a horizontal line in the series linking x_i and x_j not intersecting intermediate data height, fulfilling:

$$x_i, x_j > x_n \text{ for all } i < n < j \quad (5)$$

In this study, the time series of the solar quiet current. Sq(H) derived during the periods of the 2009 and 2021 SSW was subjected to the HVG method which transform the series into a complex network. The calculations were performed using the ts2vg Python module, specifically utilizing the HorizontalVG class, which represents one of the types of visibility graphs, namely the 'Horizontal Visibility Graph'. The input to this process is a time series, which is transformed into a network where each point in the series becomes a node, and edges are formed based on the visibility criteria between points. By applying this method, we calculate the degree (number of connections) for each point in the time series, capturing the number of other points it can 'see' in the horizontal visibility graph. The output is a list of degrees for each point, reflecting the local connectivity structure within the time series, which helps reveal patterns, dependencies, and variability within the data.

2.3 Fuzzy Entropy (FuzzyEn)

Fuzzy entropy (FuzzyEn) is a powerful and popular nonlinear tool used to assess the dynamical characteristics of time series data (Ishikawa and Mieno, 1979; Li et al., 2017; Azami et al., 2019; Chen et al., 2007). It provides a quantitative measure of a signal's complexity and chaos. High entropy indicates a more chaotic structure, whereas low entropy suggests a more regular or periodic nature. FuzzyEn was developed to overcome the shortcoming of approximate entropy (ApEn) and sample entropy (SampEn) (Azami et al., 2019; Li et al., 2017; Dass et al., 2019).

https://doi.org/10.5194/egusphere-2024-3554
Preprint. Discussion started: 20 November 2024

FuzzyEn uses exponential functions with Fuzzy boundaries. It is expressed mathematically as follows. Given a time series X_i , Eq. (4),

we embed it using a given embedding dimension (m). Then, a new m-dimensional vector (X_m) is formed as

$$X_m(i) = [X_i, X_{i+1}, \dots, X_N] - x0_i \qquad (6)$$

These vectors represent m consecutive x-values, starting with the i-th points, and with the baseline $x0_i = \frac{1}{m}\sum_{j=0}^{m-1} x_{i+j}$ removed. Then, the distance between vectors $X_m(i)$ and $X_m(j)$, $d_{i,j,m}$ can be defined as the maximum absolute difference between their scalar components. Given n and r, the degree of similarity $(D_{i\ j,m})$ of the vectors $X_m(i)$ and $X_m(j)$ is calculated using the fuzzy function.

$$D_{i,j,m} = \mu\left(d_{i,j,m}, r\right) = exp\left(\frac{-(d_{i,j,m})^n}{r}\right) \qquad (7)$$

Where n and r are the FuzzyEn power and threshold respectively. The function ϕ_m is defined as

$$\phi_m(n,r) = \frac{1}{N-m}\sum_{i=1}^{N-m}\left(\frac{1}{N-m-1}\sum_{\substack{j=1 \\ j\neq i}}^{N-m} D_{i,j,m}\right) \qquad (8)$$

Repeating the same procedure from equation (7) and equation (8) for the vector $X_{m+1}(j)$, i.e., for dimension $(m+1)$, the function ϕ_{m+1} is obtained. Therefore, FuzzyEn can be estimated as

$$\text{FuzzyEn}\ (m, n, r, N) = \ln \phi_m(n,r) - \ln \phi_{m+1}(n,r) \qquad (9)$$

In this study, we applied the FuzzyEn to the solar quiet current, Sq(H), to investigate ionospheric chaos during SSW across the Europe and Africa sector. The computational parameters used for FuzzyEn analysis included an embedding dimension $(m = 1)$ and a tolerance threshold defined as r_1=0.2×std, where std represents the standard deviation of the time series X. Additionally, the

https://doi.org/10.5194/egusphere-2024-3554
Preprint. Discussion started: 20 November 2024

argument exponent (pre-division) r_2=3 was applied, along with a time delay of τ=1. The window size used for the analysis was s=200.

The calculations were performed using Python with the EntropyHub library [EntropyHub. An Open-Source Toolkit for Entropic Time Series Analysis. Available online: https://www.entropyhub.xyz/ (accessed on 27 February 2024).] (version 0.2), which provides a reliable and standardized method for calculating FuzzyEn, ensuring that the results can be compared across different studies. EntropyHub integrates many established entropy methods into a single package, available for Python, MatLab, and Julia users. By utilizing this library, we ensured the consistency and reproducibility of our entropy calculations. The FuzzyEn was computed using the solar quiet current time series for the SSW periods of 2009 (January-March) and 2021 (December 2020-February 2021) after applying the Horizontal Visibility Graph (HVG) transformation.

https://doi.org/10.5194/egusphere-2024-3554
Preprint. Discussion started: 20 November 2024

3. Results

A sample of solar-quiet current Sq(H) on 31st of March 2009 at Addis Ababa, Ethiopia is shown in Figure 6 (a-d). The panel (a) represent the time series of the solar quiet current derived in minutes, while panel (b) is the detrended time series of solar quiet current transformed through Horizontal Visibility Graph (HVG). The panel (c) is the FuzzyEn depicting the changes in entropy of the solar quiet current without HVG transformation. The result in panel (d) depicts the changes in entropy of solar quiet current transformed through HVG. The solar quiet current gradually enhances in magnitude during the peak noon periods in its daily variation, while at pre-noon and post-noon periods, a gradual increment and a decrease in the magnitude of the solar quiet current was observed. The results of Fuzzy Entropy values after HVG transformation reveals a gradual decrease in entropy at noon-periods. Notably, during pre-noon and post-noon periods, the result revealed an increment in entropy changes. These distinct features of entropy changes obtained in Fuzzy Entropy after HVG transformation of the solar quiet time series was not obvious in the results of Fuzzy Entropy obtained without HVG transformation method. The HVG transformation series unveils the transient changes in entropy for ionospheric current system during SSW. This indicates that the HVG transformation method captures the dynamical characteristics of the ionospheric current enabling, the unveiling of chaotic behavior obtained through changes in Fuzzy Entropy during the periods of 2009 (January-March) and (December 2020-Februaury 2021) SSW events.

The day-to-day latitudinal distribution of entropy across Europe and Africa sector in January 2009 is display in Figure 7. The contour map depicts the entropy changes in color representation. The yellow color unveils ranges of Fuzzy Entropy values between 1.2 and 1.4 indicating high entropy. This high entropy indicates the presence of ionospheric chaos (disorderliness) in the ionospheric

https://doi.org/10.5194/egusphere-2024-3554
Preprint. Discussion started: 20 November 2024

current system. The light blue color ranging at approximately 1.2~0.8 reveals a declining Fuzzy Entropy value which indicates a declining to orderliness behavior in the ionospheric current system. While the deem blue color ranging at 0.8~0.6 depicts low entropy values. The low entropy indicates the presence of orderliness behavior in the ionospheric dynamics. We noticed that in the day-to-day latitudinal distribution of entropy across the stations in the Europe and Africa sector. Some days in January 2009 depicts the presence of ionospheric chaos at most of the stations shown in Figure 5. Such that high entropy values were recorded on 1st, 4th, 8th, 10th, 14th, 18th-25th and 28th-31st of January at stations IZN, SUA, KIV, BOX and SOD (see Tab. 1). On 25th of January, a higher entropy values, unveiling chaotic behavior in the ionospheric dynamics, was observed in all the investigated stations in the European and African sector. Notably, low entropy values, signifying orderliness (periodic) behavior in the dynamics of ionosphere, was observed on 3^{rd},5^{th}-7^{th}, 9^{th}, 11^{th}-16^{th}, and 26^{th} of January. The lowest entropy values were found on 3^{rd} of January, indicating that the state of the ionosphere exhibits a highly orderliness behavior in its underlying dynamics across the Europe-Africa sector during this period.

We display the contour plots of the day-to-day latitudinal distribution of entropy on February 2009 in Figure 8. The changes in entropy unveils high values of Fuzzy Entropy indicating the presence of ionospheric chaos in most of the station across the Europe and Africa sector. This trend of high entropy values was noticed on 1st-2nd, 9th-10th, 15th, 17th-18th of February. This high entropy observed in the aforementioned days signifies that the dynamics of the ionosphere is chaotic. In addition, 1^{st} and 17^{th} February exhibited even more chaotic behavior across the stations. This observation further strengthening the evident influence of SSW on the ionospheric dynamics on these dates. Notably, low entropy implying the presence of orderliness behavior in the dynamics of the ionosphere was obvious on 5^{th}-8^{th}, 11^{th}-12^{th}, 14^{th}, 16^{th}, 19^{th}-22^{nd}, and 25^{th}-27^{th} of February

https://doi.org/10.5194/egusphere-2024-3554
Preprint. Discussion started: 20 November 2024

2009. However, 5th and 14th of February exhibited the lowest entropy values, revealing that the state of the ionosphere is at a minimal perturbation state.

The day-to-day latitudinal distribution of entropy across the European and African sector on March 2009 is shown in Figure 9. Most of the Fuzzy entropy values are associated with low entropy. For instance, 1st-6th, 8th-18th, 20th-23rd, 26th-28th and 31st of March depicts low changes in entropy in most of the stations. High entropy values associated with the presence of ionospheric chaos was found on 7th, 24th, and 29th-30th of March.

The Fuzzy Entropy of the day-to-day latitudinal distribution across European sector on December 2020 is presented in Figure 10. We observed that the changes in entropy from 1st to 6th of December at the SOD, BOK and KIV stations reveals a consistently low entropy values, indicating that the state of the ionosphere at these stations exhibits a consistent orderliness behavior during these periods. However, at SUA and IZN, consistent high entropy values indicating the presence of ionospheric chaos from 1st to 5th of December was observed. Notably, on 6th of December, all the stations in the European sector (SOD, BOK, KIV, SUA, and IZN) depicts low entropy signifying that the dynamics of ionosphere is less perturbed by the influence of SSW on December 2020. However, a high entropy values indicating chaotic behavior in the ionospheric dynamics was observed at SOD, BOK, and KIV stations on 7th and 8th of December. Interestingly, SUA and IZN were consistently associated with a low entropy distribution from 8th to 22nd of December. This observed consistent low entropy at SUA and IZN signifies that the ionosphere in this region is less perturbed by the influence of SSW. Furthermore, the possible emergence of ionospheric disturbances at SUA and IZN during those observed days is extremely minimal. A consistent decline from disorderliness (chaotic) to orderliness (periodic) was observed at SOD, BOK, and

https://doi.org/10.5194/egusphere-2024-3554
Preprint. Discussion started: 20 November 2024

KIV from 25th to 31st of December, while SUA and IZN exhibited some features of ionospheric chaos on 30th and 31st of December.

For SSW January 2021, the day-to-day latitudinal distribution of entropy across Europe sector is displayed in Figure 11. The latitudinal distribution depicts low entropy across the day-to-day observation in January. For instance, 1st-6th, 8th-11th, 13th-16th, 19th-24th, and 26th-28th of January unveils low entropy values across the stations investigated in the Europe sector implying that the ionosphere at this region exhibits orderliness (periodic) behavior in its underlying dynamics. Notably, high entropy, indicating the presence of ionospheric chaos (disorderliness), was observed at SUA and IZN on 7th, 10th, and 18th of January.

In Figure 12 displaying the day-to-day latitudinal distribution of entropy in February 2021 across Europe sector. The changes in entropy reveals high entropy, suggesting the presence of ionospheric chaos on 9th, 12th, 16th-18th, 21st, and from 24th to 27th of February at SOD, BOX, SUA and IZN. In contrast, KIV consistently exhibited low values of entropy from 1st to 8th of February.

3.1 Ionospheric Chaos During Phases of 2009 SSW

Display in Figure 13 is the latitudinal distribution of entropy across Europe and Africa sector during the phases of 2009 SSW. The phases of SSW are categorized into six namely: precondition phase, ascending phase, peak phase, descending phase, after SSW phase and no SSW phase. The entropy values during the precondition phase of SSW depicts a high entropy across the stations in the Europe sector signifying that the precondition phase of 2009 SSW were associated with the emergence of ionospheric chaos. The observed features of high entropy values unveiling pronounced ionospheric chaos at SUA, KIV, BOX and SOD were obvious. This observation further reveals the emergence of ionospheric disturbances in SUA, KIV, BOX and SOD due to the

https://doi.org/10.5194/egusphere-2024-3554
Preprint. Discussion started: 20 November 2024

influence of SSW. Interestingly, the periods from January to March 2009, characterized by SSW, were strongly associated with geomagnetic quiet periods (see, Figure 2a). In the African sector, SSW preconditioning phase is characterized by a declining in entropy values, indicating that the state of the ionosphere across Africa sector is transiting to orderliness behavior in its underlying dynamics at the preconditioning phase of 2009 SSW. A low entropy was seen at AAB, NAB and DES during the preconditioning phase signifying that the underlying dynamics of the ionosphere at AAB, NAB, and DES are exhibiting orderliness as the preconditioning phase of SSW emerges. During the ascending phase of SSW, we observed also a low entropy values at stations in Africa up to IZN. However, high values of entropy implying the presence of ionospheric chaos (disorderliness) were found at KIV, BOX, and SOD. The high entropy observed at these stations during the ascending phase indicates that the influence of SSW on the state of the ionosphere at KIV, BOX, and SOD is present. This suggests that SSW events significantly affect ionospheric dynamics, leading to increased variability and changes in electron density patterns across Europe sector during the ascending phase of 2009 SSW. In the African sector, during the ascending phase of SSW, we observed that, with the exception of the ASW and KRT stations, high entropy values were recorded around 16-24hr (LT). All other stations investigated in Africa depict low entropy values. This further signifies that the ionospheric dynamics in most of the stations investigated in the Africa sector during the ascending phase exhibits orderliness (periodic) behavior in its underlying dynamics.

During the peak phase of SSW 2009, evidence of ionospheric chaos was observed at SOD, BOX and SUA. The changes in entropy during this period depicts high values, indicating significant disturbances in the ionosphere. A declining and steady low entropy change was observed from SUA to DES. In contrast, KRT, AAB and NAB exhibited very low entropy values around 4-10

https://doi.org/10.5194/egusphere-2024-3554
Preprint. Discussion started: 20 November 2024

hours (LT) during the peak phase of SSW. This observed low entropy changes at KRT, AAB and NAB signifies that the contributing influence of SSW to ionospheric dynamics at KRT, AAB and NAB is not pronounced at the peak phase of 2009 SSW compared to the stations situated in the European sector. At the descending phase of SSW, high entropy values associated with the presence of ionospheric chaos was evident at SOD, BOX, KIV, SUA, IZN, FYM and ASW. However, AAB and NAB depicts low entropy values during the descending phase unveiling that ionospheric dynamics at AAB and NAB are not influenced by SSW during this period.

The after-SSW phase of 2009 also exhibits a distribution of high entropy values across the investigated stations from the Europe to the Africa sector. Notably, at 8-16hr (LT), a declining entropy was noticed at KRT while low entropy values were seen at AAB, NAB, DES, LSK and MPT. At 20-24hr (LT), ionospheric chaos associating with high entropy was evident at LSK, DES, AAB, KRT, ASW and FYM. During the no-SSW phase, the changes in entropy were observed to decline at SOD, BOX, KIV and IZN. In contrast, at SUA high entropy values indicative for ionospheric chaos were noted. A consistent low entropy change was found in ASW, KRT, AAB, NAB, DES, LSK and MPT.

3.2 Ionospheric chaos during phases of 2021 SSW

Shown in Figure 14 is the 2021 SSW latitudinal distribution of entropy across Europe sector at precondition, ascending, peak, descending, After-SSW and no-SSW phases. The Precondition phase at SOD, BOX, and KIV depicts high values of entropy signifying that ionospheric chaos is dominant during this period, while a declining and low entropy change was observed at IZN and SUA. The ascending, peak, descending and after SSW phases exhibit a consistent low entropy value in their latitudinal distribution, suggesting orderliness behavior in the ionosphere across SOD, BOX and KIV. In contrast, at SUA a consistent increase in entropy was evident. This

https://doi.org/10.5194/egusphere-2024-3554
Preprint. Discussion started: 20 November 2024

consistent increase in entropy at SUA during all the phases of SSW implies that the ionospheric dynamics is consistently exhibiting chaotic behavior due to the influence of SSW.

4. Discussion of Results

The chaotic behavior of the ionosphere is prevailing due to the dynamical characteristics of the atmospheric layers. Evidence of chaos in the ionosphere, magnetosphere due to space weather effects have been investigated using various chaotic quantifiers such as entropy, Lyapunov exponent, correlation dimension and recurrence plot (Unnikrishnan, 2008; Pavlos et al., 1992; Pavlos, 2012; Donner et al., 2019; Ogunsua et al., 2014; Balasis et al., 2023). However, the ionospheric chaos with regards to regional information has not been ascertained, especially during extreme meteorological event such as SSW. To ascertain the degree of SSW influence on the dynamics of the regional ionosphere within 26° to 40° Eastern geographical longitude. This present study unveils the ionospheric chaos response to solar quiet current, Sq(H) dynamics across Europe and Africa sector during 2009 and 2021 SSW event. The ionospheric dynamics is a complex system, driven by a set of atmospheric elements that continually interacts with the geospace environment. They are sensitive to any small change in the atmospheric drivers that can amplify and lead the ionospheric plasma to instability (disorderliness) or stability (orderliness) from its initial state. This sensitivity defines the potential for ionospheric chaos (Marwan et al., 2007; Conejero et al., 2024; Velichko and Heidari, 2021; Boriskov et al., 2022). The chaotic behavior is strongly associated with high entropy while the orderliness behavior is associated with declining and low entropy. These features are characteristic of a dynamical system, and the ionosphere serves as a prime example of such a system (Materassi, 2020; Radicella and Nava, 2020; Hokkanen, 2000; Ogunsua et al., 2014).

https://doi.org/10.5194/egusphere-2024-3554
Preprint. Discussion started: 20 November 2024

Previous studies by (Goncharenko et al., 2010; Fejer et al., 2011; Yamazaki et al., 2012c, a; Yamazaki, 2014; Yamazaki et al., 2016; Gómez-Escolar et al., 2014; Baldwin et al., 2021; Goncharenko et al., 2021; Hocke et al., 2024; Fuller-Rowell et al., 2016; Gupta et al., 2021; Ma and Hocke, 2024) and other researchers have established the potential reshaping of ionospheric plasma associated with the emergence of SSW. Our present findings unveils the evidence of ionospheric chaos been more pronounced at SUA, KIV, BOX and SOD compared to the stations situated in the African sector. A consistent dynamics of orderliness behavior in the ionosphere was noticed at AAB, NAB and DES. Furthermore, we noticed that, as the stratospheric temperature rises, a clear orderliness behavior becomes evident in the African sector. For instance, our results unveil that low entropy begins to converge around AAB during the preconditioning phase of SSW. While at the ascending phase, the low entropy spread from AAB across MPT and FYM, the region of both Southern and Northern Hemisphere of Africa sector. Then during the SSW peak, low entropy diminishes and converges at KRT, AAB and NAB. From the SSW descending phase till No-SSW phase, we noticed that the features of low entropy begin to expand and spread across all the stations in the Africa sector. This low entropy indicative for orderliness behavior is found to be more pronounced during the no-SSW phase. Remarkably, the observation of low entropy values across all the stations situated in the Africa sector reveals that the influence of SSW to ionospheric dynamics in the Africa sector is minimal. Furthermore, the evidence of low entropy, an indicative of orderliness implies that the chaotic behavior at the regional ionosphere of Africa sector is extremely low facilitating steady dynamics of ionospheric current system during the SSW. However, ionospheric chaos was evident in most of the station situated in the Europe sector. In that, at the precondition phase of SSW, the ionospheric chaos spans from FYM till SOD while at the ascending phase, the chaotic behavior was only observable at KIV, BOX and SOD. Notably,

https://doi.org/10.5194/egusphere-2024-3554
Preprint. Discussion started: 20 November 2024

during the peak phase, the ionospheric chaos enhanced at SUA, KIV, BOX and SOD. This observed enhancement in ionospheric chaos spans further during the descending phases of SSW. At the after SSW phase, the ionospheric chaos extends to some station in the Southern Hemisphere of the Africa sector around 0-6hr (LT) in FYM, ASW, KRT, and AAB. During the no-SSW phase, the stations situated in the Europe sector exhibited a decline of ionospheric chaos at SOD, BOX, KIV and IZN. These findings of ionospheric chaos in most of the stations situated in the Europe sector unveils the evidence that the 2009 SSW indeed significantly influenced the ionospheric dynamics in this region. Interestingly, during the 2009 SSW periods, geomagnetic activities were characterized by a planetary index of $K_p \leq 2^+$ and a solar flux ($F_{10.7}$) of approximately 72 (see Figure 3). This record indicates that geomagnetic disturbances were extremely low during the 2009 SSW. Therefore, the finding that ionospheric chaos was dominant in most stations located in the European sector, compared to those in the African sector, provides additional evidence of the SSW's contributing influence on the regional ionosphere in Europe sector. In the 2021 SSW, the entropy distribution at KIV, BOX, and SOD unveils significant enhancement of ionospheric chaos during the preconditioning phase of SSW while orderliness behavior was noticed at SUA and IZN. The orderliness behavior of the ionospheric dynamics was evident during the ascending, peak and descending phase of SSW at SOD, BOX, and KIV. Then, at the after SSW and no-SSW phases, the presence of ionospheric chaos begins to emanate at SOD, BOX and KIV. Evidence of ionospheric chaos was prominent at SUA during the ascending, peak, descending, after, and no-SSW phases. This observed feature of ionospheric chaos at SUA unveils the evidence of the SSW influence on the ionospheric dynamics in some regions of the European sector during the 2021 SSW.

https://doi.org/10.5194/egusphere-2024-3554
Preprint. Discussion started: 20 November 2024

The observation of prevailing ionospheric chaos due to SSW across European sector suggest that for a relatively good predictability of SSW effects on the ionosphere. The effort of understanding the regional ionospheric chaos characteristics will enhance ionospheric forecasting skill. Because some of our findings of change in entropy associated with regional ionosphere are noticed to be less sensitive to SSW influences propagating from the lower atmosphere (See Figures 13 and 14). This observation also highlights orderliness behavior where the ionospheric disturbances due to SSW influences are relativity suppress. It is worthy to note that emergence of orderliness behavior in the ionospheric dynamics due to SSW does not completely erase chaotic behavior. Rather, it's an evidence of suppression of chaos due to SSW event. We suspect that the regions where orderliness behavior are pronounced due to SSW influences could suggest that the coupling processes between the atmospheric drivers are in strong synchrony leading to synchronization characteristics in ionospheric dynamics. For instance, in the Africa sector, stations within the equatorial region i.e. AAB consistently exhibits orderliness behavior such that low entropy values were consistently observed during the phases of SSW. This observation will be extensively research in our future investigation with primary focus on equatorial region.

The evidence of ionospheric chaos could result to the formation of small/large disturbances in the European sector owning to the impact of disruption on communication and navigation signals during SSW. This observation of ionospheric chaos may be attributed to the enhancement of the solar and lunar migrating semidiurnal tides during SSWs, which influences the generation of electric fields through the E-region dynamo mechanism (Goncharenko et al., 2021; Pedatella et al., 2014; Siddiqui et al., 2018)

https://doi.org/10.5194/egusphere-2024-3554
Preprint. Discussion started: 20 November 2024

5.0 Conclusion

This study aimed to unveil the contributing influence of Sudden Stratospheric Warming (SSW) on the regional ionosphere across Europe and Africa by examining ionospheric chaos in the solar quiet current during the SSW events of 2009 and 2021. These SSW events occurred during the solar minimum years of solar cycle 24. The SSW was categorized according to the rising stratospheric temperature into six phases namely precondition, ascending, peak, descending, after, and no-SSW phases. The study covers 13 magnetometer stations across the Europe and Africa sector located within the geographical longitude of 26° to 40° East. Magnetometer data obtained during the periods of SSW were used to derive time series of the ionospheric solar quiet current, Sq(H). These solar quiet current time series were transformed into a network representation through the Horizontal Visibility Graph (HVG) approach and analysed by Fuzzy Entropy to quantify the presence of ionospheric chaos during the periods of SSW. Low entropy is associated with orderliness behavior. We found that the latitudinal distribution of entropy depicts high entropy indicating the presence of ionospheric chaos in most of the stations situated within the Europe sector compared to stations in the Africa sector. A consistent low entropy distribution unveiling the presence of orderliness behavior was found to be prominent in the Africa sector. This prevailing evidence of orderliness behavior in the Africa sector during SSW signifies that the contribution influence of SSW to the regional ionosphere of Africa sector is minimal. However, the pronounced features of ionospheric chaos found in the Europe sector unveil the evidence of significant effects of SSW on the regional ionosphere in Europe. Finally, we found that after the peak phase of SSW, the ionospheric chaos is more pronounced.

https://doi.org/10.5194/egusphere-2024-3554
Preprint. Discussion started: 20 November 2024

Code availability

The code is a collection of routines in MATLAB (MathWorks) and is available upon request to the corresponding author.

Data availability

The magnetometer data are publicly available and provided by Magnetic Data Acquisition System (MAGDAS) at the International Research Centre for Space and Planetary Environment Science, Fukuoka, Japan (http://magdas2.serc.kyushu-u.ac.jp/). The magnetometer can also be access at the International Real-time Magnetic Observatory Network (INTERMAGNET) (available online at www.intermagnet.org). While the stratospheric temperature can be access from National Oceanic and Atmospheric Administration (NOAA) (https://psl.noaa.gov/data/getpage/). The planetary index are provided and access GFZ Indices of Global Geomagnetic Activity (https://www.gfz-potsdam.de/Kp-index/). The data of disturbance storm time in minute resolution (SYM-H) is available at the World Data Centre for Geomagnetism, Kyoto, Japan: https://wdc.kugi.kyoto-u.ac.jp/, while the solar flux index are archived at the National Aeronautics and Space Administration (NASA), Space Physics Facility: https://omniweb.gsfc.nasa.gov/form/dx1.html

Author contributions

IAO developed the idea behind the problem being solved, supervise the project, analyzed the data; developed the codes; and draft the manuscript; **VA** supervise the project, developed the codes, analyzed the data and contribute to the drafting of the manuscript; **MN** supervise the project and contribute to the drafting of the manuscript; **OOI, BOS, and OBO** contributes to the interpretation and Discussion of results; **NAN and OOT** read and made useful comments to the manuscript.

Competing interests

Some authors are members of the editorial board of nonlinear processes in geophysics journal, and the authors declare they have no conflict of interest.

Acknowledgement

The authors would like to appreciate the Magnetic Data Acquisition System (MAGDAS) for providing the magnetometer data used for this research upon the request from the project leader of MAGDAS/CPMIN observations Dr. A. Yosikawa. I also extend the author gratitude to the INTERMAGNET Networks for making available the magnetometer data across the globe.

References

Antokhina, O. Y., Antokhin, P. N., Zorkaltseva, O. S., Bobrovnikov, S. M., Zharkov, V. I., and Trifonov, D. A.: Characteristics of the dynamics and relationships of the troposphere and stratosphere in the winter period 2022-2023, 12780, 31, https://doi.org/10.1117/12.2688249, 2023.

Azami, H., Li, P., Arnold, S. E., Escudero, J., and Humeau-Heurtier, A.: Fuzzy entropy metrics for the analysis of biomedical signals: Assessment and comparison, IEEE Access, 7, 104833–104847, https://doi.org/10.1109/ACCESS.2019.2930625, 2019.

Balasis, G., Balikhin, M. A., Chapman, S. C., Consolini, G., Daglis, I. A., Donner, R. V., Kurths, J., Paluš, M., Runge, J., Tsurutani, B. T., Vassiliadis, D., Wing, S., Gjerloev, J. W., Johnson, J., Materassi, M., Alberti, T., Papadimitriou, C., Manshour, P., Boutsi, A. Z., and Stumpo, M.: Complex Systems Methods Characterizing Nonlinear Processes in the Near-Earth Electromagnetic Environment: Recent Advances and Open Challenges, Space Sci. Rev., 219,

https://doi.org/10.5194/egusphere-2024-3554
Preprint. Discussion started: 20 November 2024

https://doi.org/10.1007/s11214-023-00979-7, 2023.

Baldwin, M. P., Ayarzagüena, B., Birner, T., Butchart, N., Butler, A. H., Charlton-Perez, A. J., Domeisen, D. I. V., Garfinkel, C. I., Garny, H., Gerber, E. P., Hegglin, M. I., Langematz, U., and Pedatella, N. M.: Sudden Stratospheric Warmings, Rev. Geophys., 59, 1–37, https://doi.org/10.1029/2020RG000708, 2021.

Bolaji, O. S., Rabiu, A. B., Bello, O. R., Yoshikawa, A., Yumoto, K., Odeyemi, O. O., and Ogunmodimu, O.: Spatial variability of solar quiet fields along 96° magnetic meridian in Africa: Results from MAGDAS, J. Geophys. Res. Sp. Phys., 120, 3883–3898, https://doi.org/https://doi.org/10.1002/2014JA020728, 2015.

Bolaji, O. S., Oyeyemi, E. O., Owolabi, O. P., Yamazaki, Y., Rabiu, A. B., Okoh, D., Fujimoto, A., Amory-Mazaudier, C., Seemala, G. K., Yoshikawa, A., and Onanuga, O. K.: Solar quiet current response in the African sector due to a 2009 sudden stratospheric warming event, J. Geophys. Res. Sp. Phys., 121, 8055–8065, https://doi.org/10.1002/2016JA022857, 2016a.

Bolaji, O. S., Oyeyemi, E. O., Owolabi, O. P., Yamazaki, Y., Rabiu, A. B., Okoh, D., Fujimoto, A., Amory-Mazaudier, C., Seemala, G. K., Yoshikawa, A., and Onanuga, O. K.: Solar quiet current response in the African sector due to a 2009 sudden stratospheric warming event, J. Geophys. Res. Sp. Phys., 121, 8055–8065, https://doi.org/https://doi.org/10.1002/2016JA022857, 2016b.

Boriskov, P., Velichko, A., Shilovsky, N., and Belyaev, M.: Bifurcation and Entropy Analysis of a Chaotic Spike Oscillator Circuit Based on the S-Switch, Entropy, 24, https://doi.org/10.3390/e24111693, 2022.

Butler, A. H., Seidel, D. J., Hardiman, S. C., Butchart, N., Birner, T., and Match, A.: Defining sudden stratospheric warmings, Bull. Am. Meteorol. Soc., 96, 1913–1928, https://doi.org/10.1175/BAMS-D-13-00173.1, 2015.

Charles Owolabi and Babatunde Rabiu and Kayode Oluyo: The Asymmetrical Behaviour of the Sq H Current Systemduring the Prenoon-Postnoon Epochs at African Longitudes, Jour. Aerosp. Sci. Technol., 1, 9–17, https://doi.org/10.17265/2332-8258/2015.01.002, 2015.

Chau, J. L., Goncharenko, L. P., Fejer, B. G., and Liu, H. L.: Equatorial and low latitude ionospheric effects during sudden stratospheric warming events : Ionospheric effects during SSW events, Space Sci. Rev., 168, 385–417, https://doi.org/10.1007/s11214-011-9797-5, 2012.

Chen, W., Wang, Z., Xie, H., and Yu, W.: Characterization of Surface EMG Signal Based on Fuzzy Entropy, IEEE Trans. Neural Syst. Rehabil. Eng., 15, 266–272, https://doi.org/10.1109/TNSRE.2007.897025, 2007.

Conejero, J. A., Velichko, A., Garibo-i-Orts, Ò., Izotov, Y., and Pham, V. T.: Exploring the Entropy-Based Classification of Time Series Using Visibility Graphs from Chaotic Maps, Mathematics, 12, https://doi.org/10.3390/math12070938, 2024.

Dass, B., Tomar, V. P., and Kumar, K.: Fuzzy entropy with order and degree for intuitionistic fuzzy set, AIP Conf. Proc., 2142, https://doi.org/10.1063/1.5122619, 2019.

Donner, R. V, Balasis, G., Stolbova, V., Georgiou, M., Wiedermann, M., and Kurths, J.: Recurrence-Based Quantification of Dynamical Complexity in the Earth's Magnetosphere at Geospace Storm Timescales, J. Geophys. Res. Sp. Phys., 124, 90–108, https://doi.org/https://doi.org/10.1029/2018JA025318, 2019.

Ern, M., Diallo, M., Preusse, P., Mlynczak, M. G., Schwartz, M. J., Wu, Q., and Riese, M.: The

https://doi.org/10.5194/egusphere-2024-3554
Preprint. Discussion started: 20 November 2024

semiannual oscillation (SAO) in the tropical middle atmosphere and its gravity wave driving in reanalyses and satellite observations, Atmos. Chem. Phys., 21, 13763–13795, https://doi.org/10.5194/acp-21-13763-2021, 2021.

Eswaraiah, S., Kim, Y. H., Liu, H., Ratnam, M. V., and Lee, J.: Do minor sudden stratospheric warmings in the Southern Hemisphere (SH) impact coupling between stratosphere and mesosphere-lower thermosphere (MLT) like major warmings? 3. Space science, Earth, Planets Sp., 69, 4–11, https://doi.org/10.1186/s40623-017-0704-5, 2017.

Fejer, B. G., Tracy, B. D., Olson, M. E., and Chau, J. L.: Enhanced lunar semidiurnal equatorial vertical plasma drifts during sudden stratospheric warmings, Geophys. Res. Lett., 38, https://doi.org/https://doi.org/10.1029/2011GL049788, 2011.

Fortin, A.: The Impact of a Changing Climate on the Frequency of Sudden Stratospheric Warming Events, 2017.

Fuller-Rowell, T. J., Fang, T.-W., Wang, H., Matthias, V., Hoffmann, P., Hocke, K., and Studer, S.: Impact of Migrating Tides on Electrodynamics During the January 2009 Sudden Stratospheric Warming, in: Ionospheric Space Weather, 163–174, https://doi.org/https://doi.org/10.1002/9781118929216.ch14, 2016.

Gómez-Escolar, M., Calvo, N., Barriopedro, D., and Fueglistaler, S.: Tropical response to stratospheric sudden warmings and its modulation by the QBO, J. Geophys. Res., 119, 7382–7395, https://doi.org/10.1002/2013JD020560, 2014.

Gonçalves, B. A., Carpi, L., Rosso, O. A., and Ravetti, M. G.: Time series characterization via horizontal visibility graph and Information Theory, Phys. A Stat. Mech. its Appl., 464, 93–102, https://doi.org/10.1016/j.physa.2016.07.063, 2016.

Goncharenko, L. P., Chau, J. L., Liu, H.-L., and Coster, A. J.: Unexpected connections between the stratosphere and ionosphere, Geophys. Res. Lett., 37, https://doi.org/https://doi.org/10.1029/2010GL043125, 2010.

Goncharenko, L. P., Coster, A. J., Plumb, R. A., and Domeisen, D. I. V: The potential role of stratospheric ozone in the stratosphere-ionosphere coupling during stratospheric warmings, Geophys. Res. Lett., 39, https://doi.org/https://doi.org/10.1029/2012GL051261, 2012.

Goncharenko, L. P., Harvey, V. L., Liu, H., and Pedatella, N. M.: Sudden Stratospheric Warming Impacts on the Ionosphere-Thermosphere System: A Review of Recent Progress, 369–400 pp., https://doi.org/10.1002/9781119815617.ch16, 2021.

Gordiyenko, G., Yakovets, A., Litvinov, Y., and Andreev, A.: The Influence of Sudden Stratospheric Warming on the Development of Ionospheric Storms: The Alma-Ata Ground-Based Ionosonde Observations, Atmosphere (Basel)., 15, https://doi.org/10.3390/atmos15060626, 2024.

Gupta, S., Upadhayaya, A. K., and Siingh, D.: Ionospheric Response to Sudden Stratospheric Warming Events Across Longitudes During Solar Cycle 24, J. Geophys. Res. Sp. Phys., 126, 1–21, https://doi.org/10.1029/2021JA029206, 2021.

Hajra, R., Tsurutani, B. T., Echer, E., Gonzalez, W. D., Brum, C. G. M., Vieira, L. E. A., and Santolik, O.: Relativistic electron acceleration during HILDCAA events: are precursor CIR magnetic storms important?, Earth, Planets Sp., 67, 109, https://doi.org/10.1186/s40623-015-0280-5, 2015.

Hocke, K., Wang, W., and Ma, G.: Influences of sudden stratospheric warmings on the ionosphere above Okinawa, Atmos. Chem. Phys., 24, 5837–5846, https://doi.org/10.5194/acp-

https://doi.org/10.5194/egusphere-2024-3554
Preprint. Discussion started: 20 November 2024

24-5837-2024, 2024.

Hokkanen, J. E. I.: Chaotic or periodic variation? Looking at Crustacea hearts, J. Theor. Biol., 203, 451–454, https://doi.org/10.1006/jtbi.2000.1096, 2000.

Hysell, D. L.: Chapter 11 - From instability to irregularities, edited by: Materassi, M., Forte, B., Coster, A. J., and Skone, S. B. T.-T. D. I., Elsevier, 137–167, https://doi.org/https://doi.org/10.1016/B978-0-12-814782-5.00011-X, 2020.

Ishikawa, A. and Mieno, H.: The fuzzy entropy concept and its application, Fuzzy Sets Syst., 2, 113–123, https://doi.org/10.1016/0165-0114(79)90020-4, 1979.

Klimenko, M. V., Bessarab, F. S., Sukhodolov, T. V., Klimenko, V. V., Koren'kov, Y. N., Zakharenkova, I. E., Chirik, N. V., Vasil'ev, P. A., Kulyamin, D. V., Shmidt, K., Funke, B., and Rozanov, E. V.: Ionospheric Effects of the Sudden Stratospheric Warming in 2009: Results of Simulation with the First Version of the EAGLE Model, Russ. J. Phys. Chem. B, 12, 760–770, https://doi.org/10.1134/S1990793118040103, 2018.

Klimenko, M. V., Klimenko, V. V., Bessarab, F. S., Sukhodolov, T. V., Vasilev, P. A., Karpov, I. V., Korenkov, Y. N., Zakharenkova, I. E., Funke, B., and Rozanov, E. V.: Identification of the mechanisms responsible for anomalies in the tropical lower thermosphere/ionosphere caused by the January 2009 sudden stratospheric warming, J. Sp. Weather Sp. Clim., 9, https://doi.org/10.1051/swsc/2019037, 2019.

Lapenta, G.: Chapter 8 - Space weather: Variability in the Sun-Earth connection, edited by: Materassi, M., Forte, B., Coster, A. J., and Skone, S. B. T.-T. D. I., Elsevier, 61–85, https://doi.org/https://doi.org/10.1016/B978-0-12-814782-5.00008-X, 2020.

Li, C., Li, Z., Guan, L., Qi, P., Si, J., and Hao, B.: Measuring the complexity of chaotic time series by fuzzy entropy, ACM Int. Conf. Proceeding Ser., Part F1305, https://doi.org/10.1145/3102304.3102320, 2017.

Li, Y., Kirchengast, G., Schwaerz, M., and Yuan, Y.: Monitoring sudden stratospheric warmings under climate change since 1980 based on reanalysis data verified by radio occultation, 40, 1259–1284, 2023.

Lin, D., Wang, W., Merkin, V. G., Huang, C., Oppenheim, M., Sorathia, K., Pham, K., Michael, A., Bao, S., Wu, Q., Zhang, Y., Wiltberger, M., Toffoletto, F., Lyon, J., and Garretson, J.: Origin of Dawnside Subauroral Polarization Streams During Major Geomagnetic Storms, AGU Adv., 3, https://doi.org/10.1029/2022AV000708, 2022.

Liu, H.-L., Wang, W., Richmond, A. D., and Roble, R. G.: Ionospheric variability due to planetary waves and tides for solar minimum conditions, J. Geophys. Res. Sp. Phys., 115, https://doi.org/https://doi.org/10.1029/2009JA015188, 2010.

Luque, B., Lacasa, L., Ballesteros, F., and Luque, J.: Horizontal visibility graphs: Exact results for random time series, Phys. Rev. E, 80, 46103, https://doi.org/10.1103/PhysRevE.80.046103, 2009.

Ma, G. and Hocke, K.: Effects of sudden stratospheric warmings on the global ionospheric total electron content using a machine learning analysis, 1–24, 2024.

Marwan, N., Carmen Romano, M., Thiel, M., and Kurths, J.: Recurrence plots for the analysis of complex systems, Phys. Rep., 438, 237–329, https://doi.org/https://doi.org/10.1016/j.physrep.2006.11.001, 2007.

https://doi.org/10.5194/egusphere-2024-3554
Preprint. Discussion started: 20 November 2024

Materassi, M.: Chapter 14 - The complex ionosphere, edited by: Materassi, M., Forte, B., Coster, A. J., and Skone, S. B. T.-T. D. I., Elsevier, 199–222, https://doi.org/https://doi.org/10.1016/B978-0-12-814782-5.00014-5, 2020.

Maute, A., Hagan, M. E., Richmond, A. D., and Roble, R. G.: TIME-GCM study of the ionospheric equatorial vertical drift changes during the 2006 stratospheric sudden warming, J. Geophys. Res. Sp. Phys., 119, 1287–1305, https://doi.org/https://doi.org/10.1002/2013JA019490, 2014.

O'Pella, J.: Horizontal visibility graphs are uniquely determined by their directed degree sequence, Phys. A Stat. Mech. its Appl., 536, 120923, https://doi.org/10.1016/j.physa.2019.04.159, 2019.

Ogunsua, B. O., Laoye, J. A., Fuwape, I. A., and Rabiu, A. B.: Nonlinear Processes in Geophysics The comparative study of chaoticity and dynamical complexity of the low-latitude ionosphere , over Nigeria , during quiet and disturbed days, 127–142, https://doi.org/10.5194/npg-21-127-2014, 2014.

Oludehinwa, I. A., Velichko, A., Ogunsua, B. O., Olusola, O. I., and Odeyemi, O. O.: Dynamical Complexity Transitions During High-Intensity Long Duration Continuous Auroral Activities (HILDCAA) Events : Feature Analysis Based on Neural Network Entropy, 1–14, https://doi.org/10.1029/2023SW003475, 2023.

Pavlos, G. P.: Magnetospheric Dynamics and Chaos Theory, 2012.

Pavlos, G. P., Rigas, A. G., Dialetis, D., Sarris, E. T., Karakatsanis, L. P., and Tsonis, A. A.: Evidence for Chaotic Dynamics in the Outer Solar Plasma and the Earth Magnetosphere BT - Chaotic Dynamics: Theory and Practice, edited by: Bountis, T., Springer US, Boston, MA, 327–

https://doi.org/10.5194/egusphere-2024-3554
Preprint. Discussion started: 20 November 2024

339, https://doi.org/10.1007/978-1-4615-3464-8_30, 1992.

Pedatella, N. M. and Forbes, J. M.: Evidence for stratosphere sudden warming-ionosphere coupling due to vertically propagating tides, Geophys. Res. Lett., 37, https://doi.org/https://doi.org/10.1029/2010GL043560, 2010.

Pedatella, N. M., Liu, H.-L., Sassi, F., Lei, J., Chau, J. L., and Zhang, X.: Ionosphere variability during the 2009 SSW: Influence of the lunar semidiurnal tide and mechanisms producing electron density variability, J. Geophys. Res. Sp. Phys., 119, 3828–3843, https://doi.org/https://doi.org/10.1002/2014JA019849, 2014.

Radicella, S. M. and Nava, B.: Chapter 6 - Empirical ionospheric models, edited by: Materassi, M., Forte, B., Coster, A. J., and Skone, S. B. T.-T. D. I., Elsevier, 39–53, https://doi.org/https://doi.org/10.1016/B978-0-12-814782-5.00006-6, 2020.

Raeder, J., Cramer, W. D., Jensen, J., Fuller-Rowell, T., Maruyama, N., Toffoletto, F., and Vo, H.: Sub-Auroral Polarization Streams: A complex interaction between the magnetosphere, ionosphere, and thermosphere, J. Phys. Conf. Ser., 767, https://doi.org/10.1088/1742-6596/767/1/012021, 2016.

Richmond, A. D.: Modeling the ionosphere wind dynamo: A review, pure Appl. Geophys., 131, 413–435, https://doi.org/10.1007/BF00876837, 1989.

Siddiqui, T. A., Maute, A., Pedatella, N., Yamazaki, Y., Lühr, H., and Stolle, C.: On the variability of the semidiurnal solar and lunar tides of the equatorial electrojet during sudden stratospheric warmings, Ann. Geophys., 36, 1545–1562, https://doi.org/10.5194/angeo-36-1545-2018, 2018.

Simons, S., Espino, P., and Abásolo, D.: Fuzzy Entropy analysis of the electroencephalogram in patients with Alzheimer's disease: Is the method superior to Sample Entropy?, Entropy, 20, 1–13, https://doi.org/10.3390/e20010021, 2018.

Takens, F.: Detecting strange attractors in turbulence BT - Dynamical Systems and Turbulence, Warwick 1980, 366–381, 1981.

Tsurutani, B. T., Lakhina, G. S., and Hajra, R.: The physics of space weather/solar-terrestrial physics (STP): What we know now and what the current and future challenges are, Nonlinear Process. Geophys., 27, 75–119, https://doi.org/10.5194/npg-27-75-2020, 2020.

Unnikrishnan, K.: Comparison of chaotic aspects of magnetosphere under various physical conditions using AE index time series, Ann. Geophys., 26, 941–953, https://doi.org/10.5194/angeo-26-941-2008, 2008.

Velichko, A. and Heidari, H.: A Method for Estimating the Entropy of Time Series Using Artificial Neural Networks, https://doi.org/10.3390/e23111432, 2021.

Velichko, A., Belyaev, M., Wagner, M. P., and Taravat, A.: Entropy Approximation by Machine Learning Regression: Application for Irregularity Evaluation of Images in Remote Sensing, Remote Sens., 14, https://doi.org/10.3390/rs14235983, 2022.

Velichko, A., Boriskov, P., Belyaev, M., and Putrolaynen, V.: A Bio-Inspired Chaos Sensor Model Based on the Perceptron Neural Network: Machine Learning Concept and Application for Computational Neuro-Science, Sensors, 23, https://doi.org/10.3390/s23167137, 2023.

Wagner, C.-U., Möhlmann, D., Schäfer, K., Mishin, V. M., and Matveev, M. I.: Large-scale electric fields and currents and related geomagnetic variations in the quiet plasmasphere, Space

https://doi.org/10.5194/egusphere-2024-3554
Preprint. Discussion started: 20 November 2024

Sci. Rev., 26, 391–446, https://doi.org/10.1007/BF00217388, 1980.

Wang, J. C., Palo, S. E., Forbes, J. M., Marino, J., Moffat-Griffin, T., and Mitchell, N. J.: Unusual Quasi 10-Day Planetary Wave Activity and the Ionospheric Response During the 2019 Southern Hemisphere Sudden Stratospheric Warming, J. Geophys. Res. Sp. Phys., 126, 1–20, https://doi.org/10.1029/2021JA029286, 2021.

Wang, Y., Li, Y., Wang, G., Yuan, Y., and Geng, H.: Influences of Sudden Stratospheric Warming Events on Tropopause Based on GNSS Radio Occultation Data, Atmosphere (Basel)., 14, https://doi.org/10.3390/atmos14101553, 2023.

Williams, R. S., Hegglin, M. I., Jöckel, P., Garny, H., and Shine, K. P.: Air quality and radiative impacts of downward-propagating sudden stratospheric warmings (SSWs), Atmos. Chem. Phys., 24, 1389–1413, https://doi.org/10.5194/acp-24-1389-2024, 2024.

Wright, C. J., Hall, R. J., Banyard, T. P., Hindley, N. P., Krisch, I., Mitchell, D. M., and Seviour, W. J. M.: Dynamical and surface impacts of the January 2021 sudden stratospheric warming in novel Aeolus wind observations, MLS and ERA5, Weather Clim. Dyn., 2, 1283–1301, https://doi.org/10.5194/wcd-2-1283-2021, 2021.

Yamazaki, Y.: Solar and lunar ionospheric electrodynamic effects during stratospheric sudden warmings, J. Atmos. Solar-Terrestrial Phys., 119, 138–146, https://doi.org/10.1016/j.jastp.2014.08.001, 2014.

Yamazaki, Y. and Maute, A.: Sq and EEJ—A Review on the Daily Variation of the Geomagnetic Field Caused by Ionospheric Dynamo Currents, Space Sci. Rev., 206, 299–405, https://doi.org/10.1007/s11214-016-0282-z, 2017.

https://doi.org/10.5194/egusphere-2024-3554
Preprint. Discussion started: 20 November 2024

Yamazaki, Y. and Richmond, A. D.: A theory of ionospheric response to upward-propagating tides: Electrodynamic effects and tidal mixing effects, J. Geophys. Res. Sp. Phys., 118, 5891–5905, https://doi.org/https://doi.org/10.1002/jgra.50487, 2013.

Yamazaki, Y., Yumoto, K., Uozumi, T., and Cardinal, M. G.: Intensity variations of the equivalent S current system along the 210° magnetic meridian, J. Geophys. Res. Sp. Phys., 116, https://doi.org/https://doi.org/10.1029/2011JA016632, 2011.

Yamazaki, Y., Yumoto, K., McNamara, D., Hirooka, T., Uozumi, T., Kitamura, K., Abe, S., and Ikeda, A.: Ionospheric current system during sudden stratospheric warming events, J. Geophys. Res. Sp. Phys., 117, 1–7, https://doi.org/10.1029/2011JA017453, 2012a.

Yamazaki, Y., Richmond, A. D., Liu, H., Yumoto, K., and Tanaka, Y.: Sq current system during stratospheric sudden warming events in 2006 and 2009, J. Geophys. Res. Sp. Phys., 117, https://doi.org/https://doi.org/10.1029/2012JA018116, 2012b.

Yamazaki, Y., Richmond, A. D., and Yumoto, K.: Stratospheric warmings and the geomagnetic lunar tide: 1958–2007, J. Geophys. Res. Sp. Phys., 117, https://doi.org/https://doi.org/10.1029/2012JA017514, 2012c.

Yamazaki, Y., Häusler, K., and Wild, J. A.: Day-to-day variability of midlatitude ionospheric currents due to magnetospheric and lower atmospheric forcing, J. Geophys. Res. Sp. Phys., 121, 7067–7086, https://doi.org/https://doi.org/10.1002/2016JA022817, 2016.

Yamazaki, Y., Matthias, V., Miyoshi, Y., Stolle, C., Siddiqui, T., Kervalishvili, G., Laštovička, J., Kozubek, M., Ward, W., Themens, D. R., Kristoffersen, S., and Alken, P.: September 2019 Antarctic Sudden Stratospheric Warming: Quasi-6-Day Wave Burst and Ionospheric Effects, Geophys. Res. Lett., 47, 1–12, https://doi.org/10.1029/2019GL086577, 2020.

https://doi.org/10.5194/egusphere-2024-3554
Preprint. Discussion started: 20 November 2024

Yasyukevich, A. S., Chernigovskaya, M. A., Shpynev, B. G., Khabituev, D. S., and Yasyukevich, Y. V.: Features of Winter Stratosphere Small-Scale Disturbance during Sudden Stratospheric Warmings, Remote Sens., 14, https://doi.org/10.3390/rs14122798, 2022.

Yiğit, E., Gann, A. L., Medvedev, A. S., Gasperini, F., Wu, Q., and Sakib, M. N.: Observation of vertical coupling during a major sudden stratospheric warming by ICON and GOLD: a case study of the 2020/2021 warming event, Front. Astron. Sp. Sci., 11, 1–16, https://doi.org/10.3389/fspas.2024.1384196, 2024.

Zhou, B., Yi, W., Xue, X., Ye, H., Zeng, J., Li, G., Tsutsumi, M., Gulbrandsen, N., Chen, T., and Dou, X.: Impact of sudden stratospheric warmings on the neutral density, temperature and wind in the MLT region, Front. Astron. Sp. Sci., 10, 1–9, https://doi.org/10.3389/fspas.2023.1192985, 2023.

Zou, S., Moldwin, M. B., Ridley, A. J., Nicolls, M. J., Coster, A. J., Thomas, E. G., and Ruohoniemi, J. M.: On the generation/decay of the storm-enhanced density plumes: Role of the convection flow and field-aligned ion flow, J. Geophys. Res. Sp. Phys., 119, 8543–8559, https://doi.org/https://doi.org/10.1002/2014JA020408, 2014.

Zou, Y., Donner, R. V., Marwan, N., Donges, J. F., and Kurths, J.: Complex network approaches to nonlinear time series analysis, Phys. Rep., 787, 1–97, https://doi.org/10.1016/j.physrep.2018.10.005, 2019.

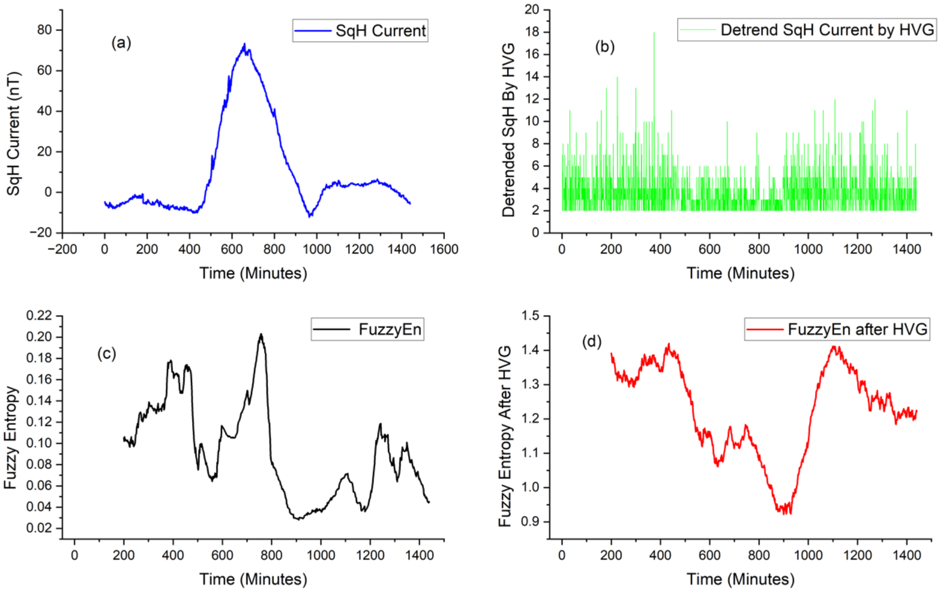

Figure 6: The sample of solar quiet current Sq(H) on 31st of March 2009 at Addis Ababa, Ethiopa: (a) The time series of solar quiet current, Sq(H) derived in minutes, (b) The detrended time series of solar quiet current transformed through Horizontal Visibility Graph (HVG), (c) The changes in Fuzzy Entropy of solar quiet current without HVG transformation, (d) The changes in Fuzzy Entropy of solar quiet current with HVG transformation.

https://doi.org/10.5194/egusphere-2024-3554
Preprint. Discussion started: 20 November 2024

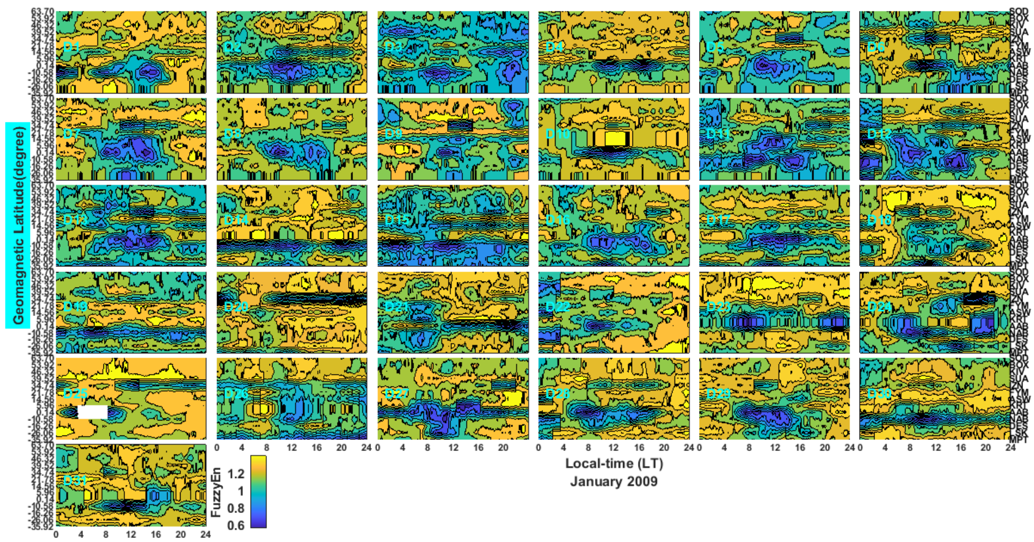

Figure 7: The Day-to-Day latitudinal Distribution of Fuzzy Entropy across Europe-Africa sector on January 2009

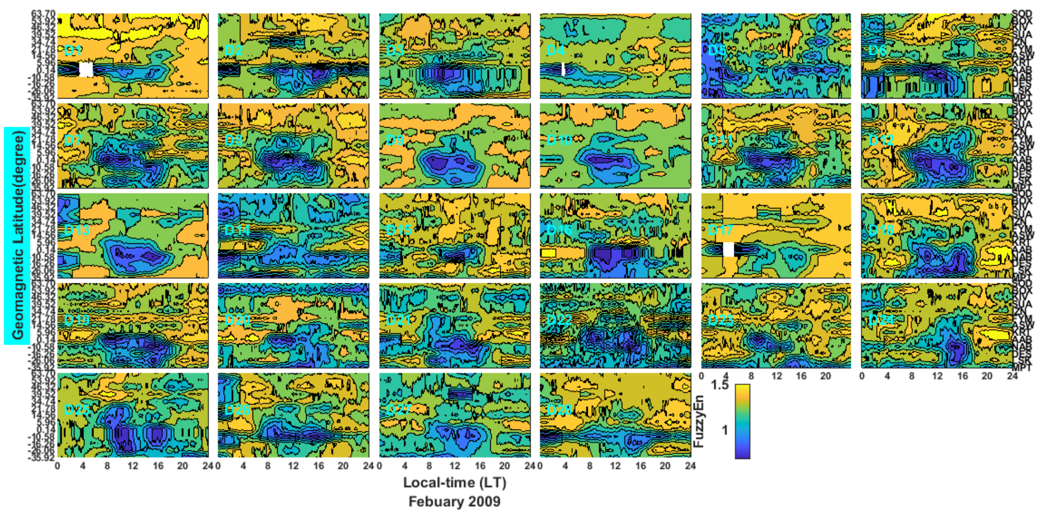

Figure 8: The Day-to-Day latitudinal Distribution of Fuzzy Entropy across Europe-Africa sector on February 2009.

https://doi.org/10.5194/egusphere-2024-3554
Preprint. Discussion started: 20 November 2024

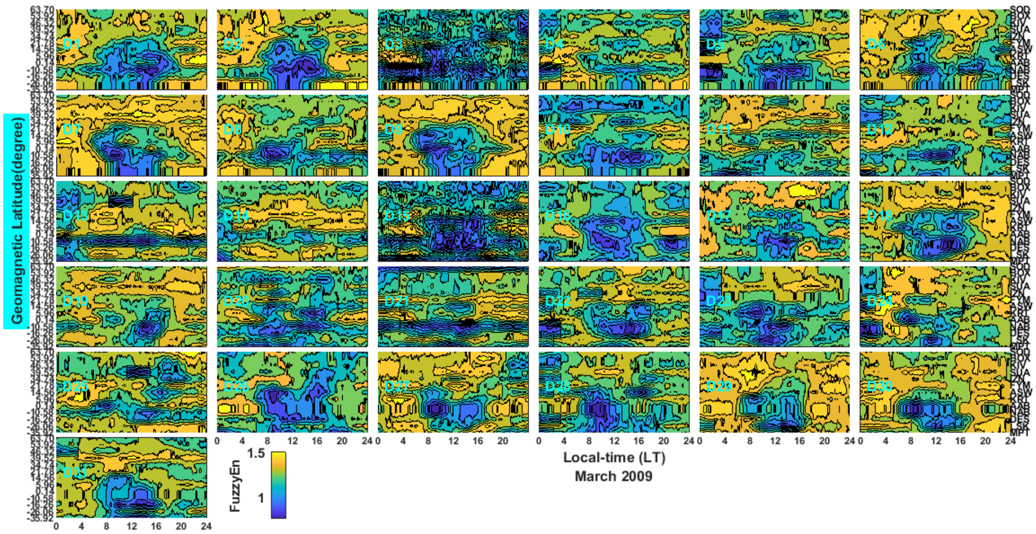

Figure 9: The Day-to-Day latitudinal Distribution of Fuzzy Entropy across Europe-Africa sector on March 2009

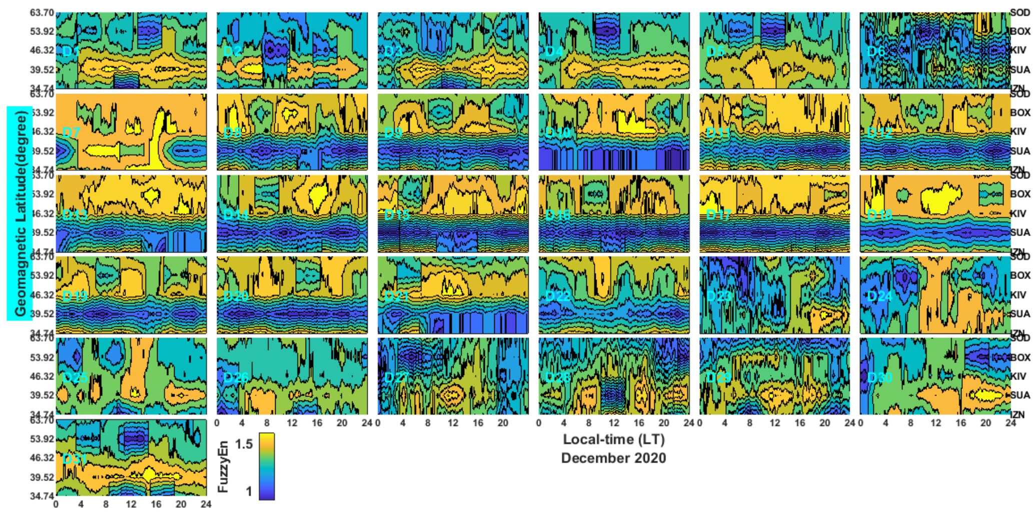

Figure 10: The Day-to-Day latitudinal Distribution of Fuzzy Entropy across Europe sector on December 2020

https://doi.org/10.5194/egusphere-2024-3554
Preprint. Discussion started: 20 November 2024

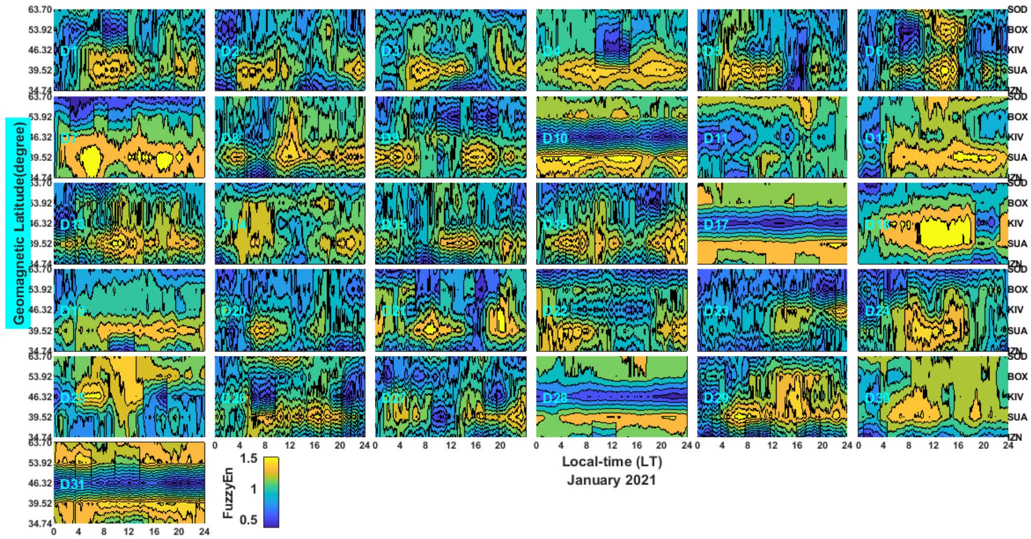

Figure 11: The Day-to-Day latitudinal Distribution of Fuzzy Entropy across Europe sector on January 2021.

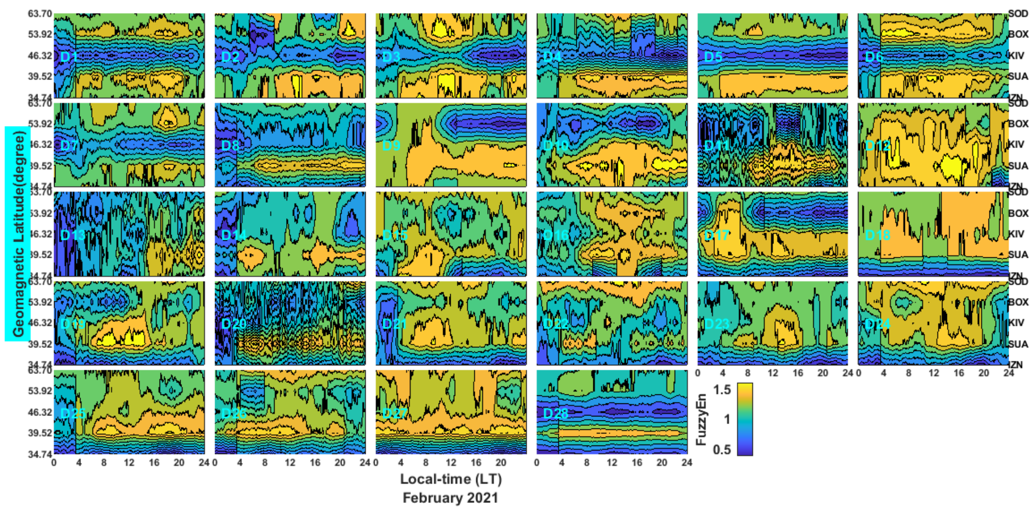

Figure 12: The Day-to-Day latitudinal Distribution of Fuzzy Entropy across Europe sector on February 2021.

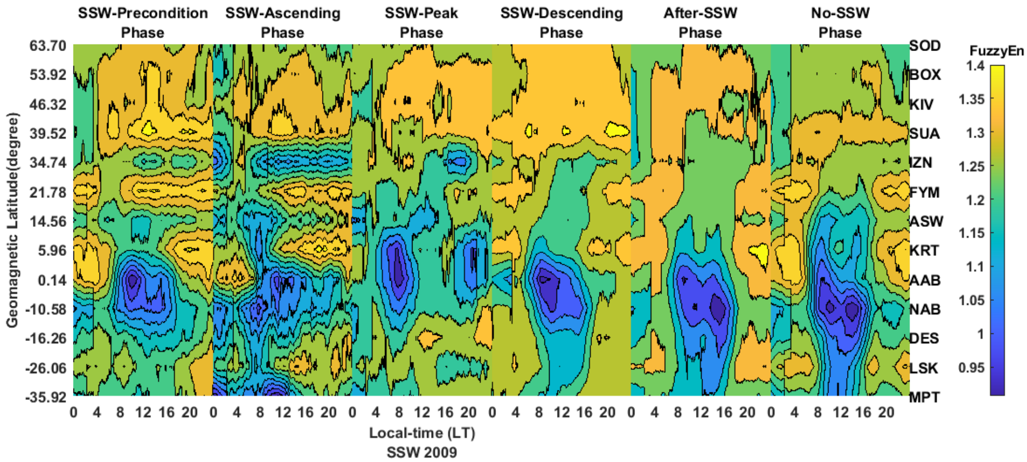

Figure 13: The latitudinal distribution of Fuzzy Entropy across Europe-Africa sector during the phases of 2009 SSW.

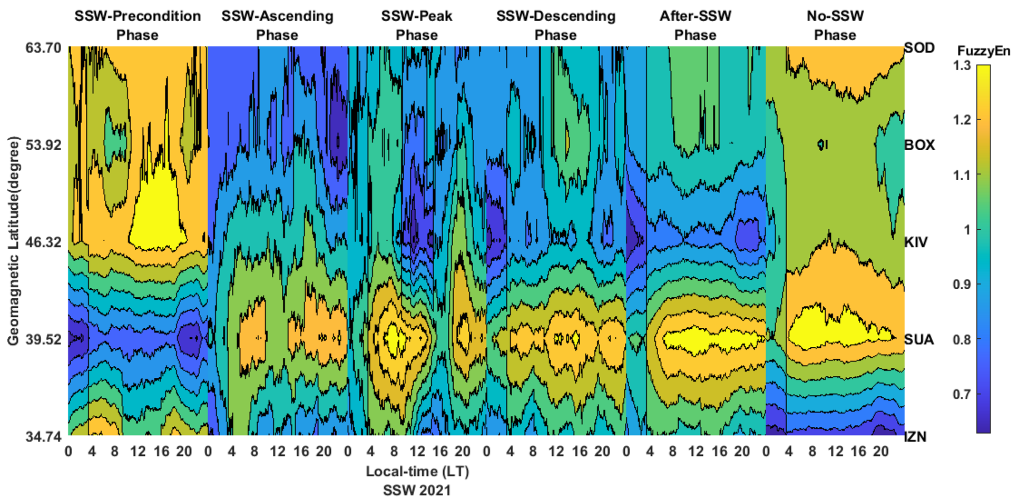

Figure 14: The latitudinal distribution of Fuzzy Entropy across Europe sector during the phases of 2021 SSW.